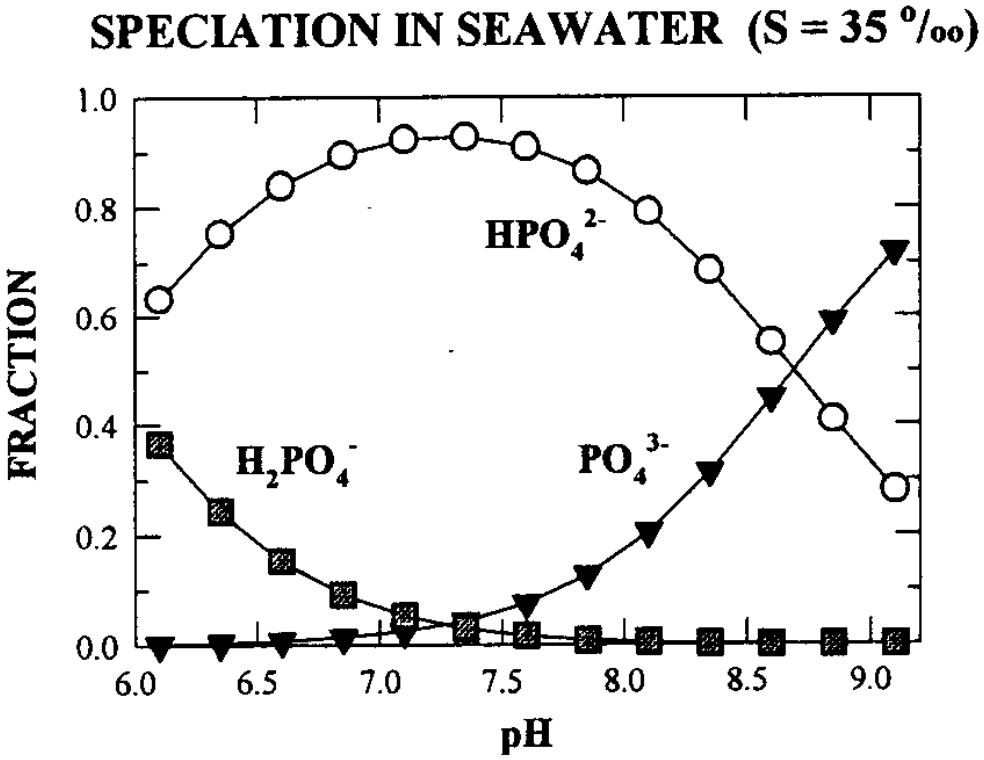

FIGURE 8.1. The various forms of phosphoric acid in water, NaCl (0.7 M), and seawater.

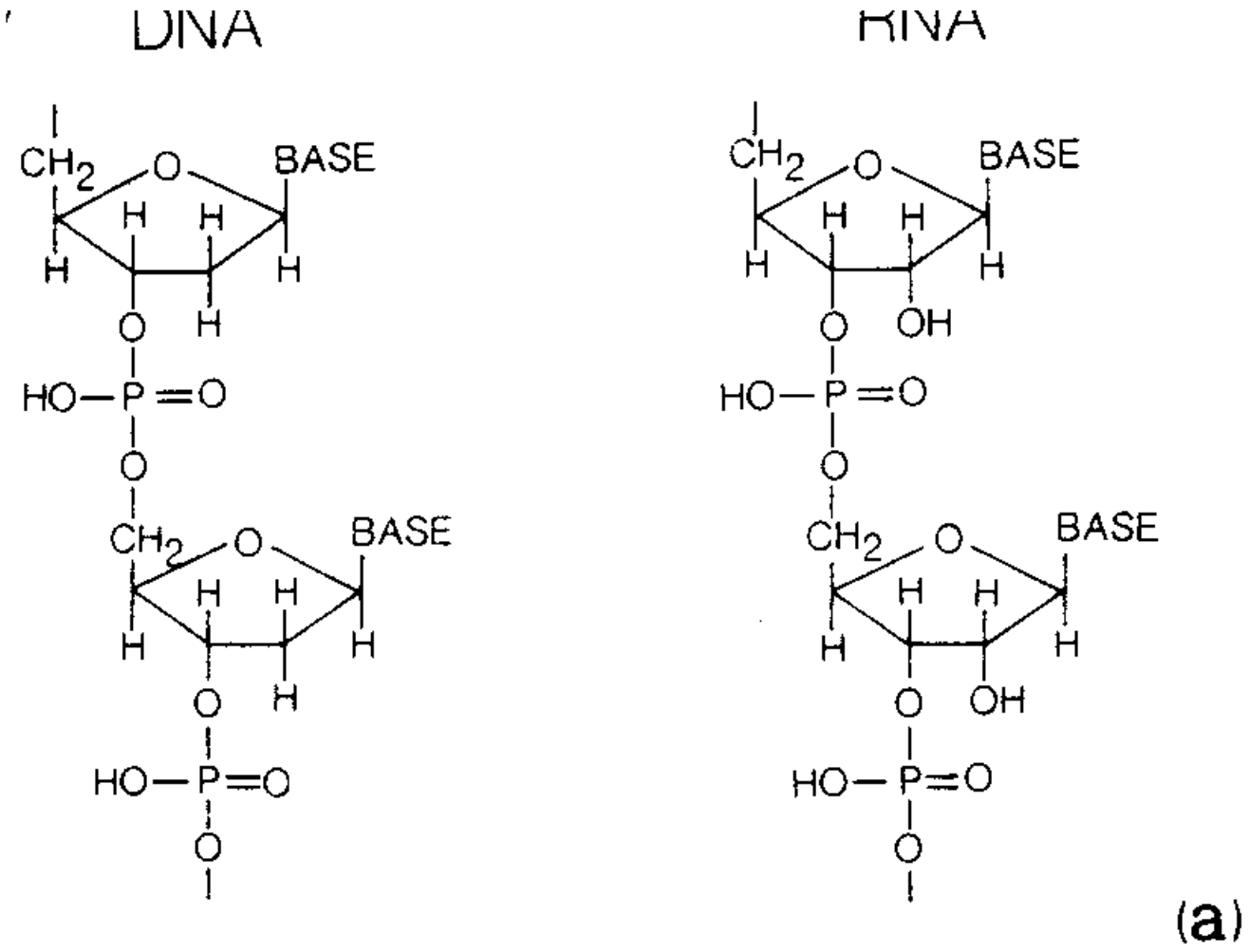
DNA
RNA
CH2
O
BASE
H
OH
HO—P=O
(a)

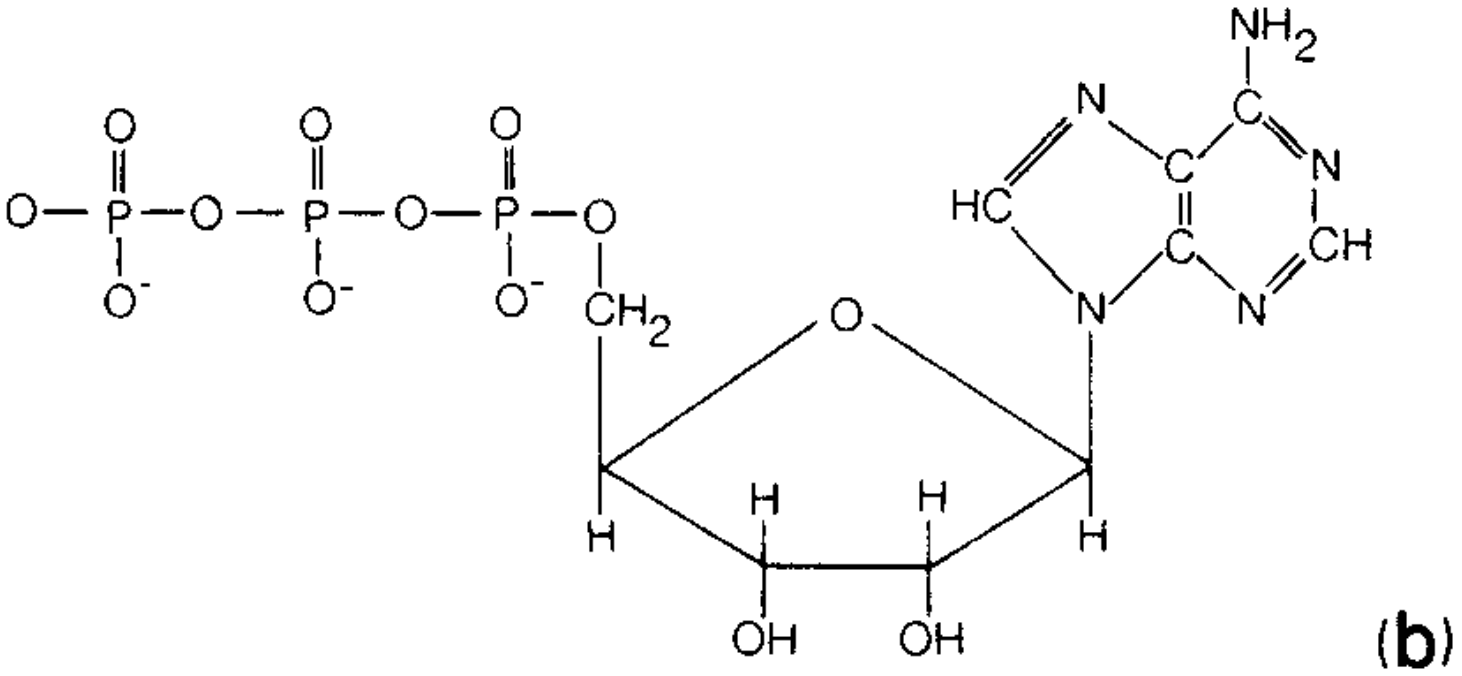

Fig. 14-3 Structure of RNA and DNA (a) and ATP (b).

Table 2
Composition of SNP in the marine environment

SNP compound class	%Composition (method)[a]	Reference
Bulk SNP		
Monophosphate Esters	10–100% (Enzymatic Assays)	Strickland and Solorzano, 1966; Kobori and Taga, 1978; Taft et al., 1977; Chrost et al., 1986
	55–77% (0–100 m; Modified UV oxidation)	Karl and Yanagi, 1997
	50% (> 100 m; Modified UV oxidation)	
Nucleotides and nucleic acids	23–45% (0–100 m; ≈ Persulfate — modified UV)	Karl and Yanagi, 1997
	50% (> 100 m; ≈ Persulfate — modifiedUV)	
	10–100% (Enzymatic Assays)	Strickland and Solorzano, 1966; Kobori and Taga, 1978; Taft et al., 1977; Chrost et al., 1986
	ATP: < 1% (Firefly bioluminescence)	Azam and Hodson, 1977; Azam et al., 1979; Hodson et al., 1981; Nawrocki and Karl, 1989
	DNA/RNA: < 5% (Multiple methods)	DeFlaun et al., 1986; Paul et al., 1986; Karl and Bailiff, 1989
Phospholipids	3–11% (Cross Flow Filtration (CFF) and Polymyxin B treatment)	Suzumura et al., 1998
Phosphonates	5–10% (^{31}P NMR)	Clark et al., 1998
Polyphosphates	0–50% (≈ Acid Reflux — UV oxidation)	Armstrong and Tibbets, 1968; Solorzano and Strickland, 1968; Solorzano, 1978
Size fractionated SNP		
LMW (< 10 kDa)	50–80% (CFF)	Matsuda 1985; Ridal and Moore, 1990; Suzumura et al., 1998
HMW (> 10 kDa)	20–50% (CFF)	Matsuda et al., 1985; Ridal and Moore, 1990;
HMW (> 50 kDa)	15% (CFF)	Suzumura et al., 1998
Monophosphate esters	10% (Alkaline phosphatase treatment)	Suzumura et al., 1998
	75% (^{31}P NMR)	Clark et al., 1998
Nucleic acids	25% (Phosphodisterase treatment)	Suzumura et al., 1998
Phospholipids	38–46% (Polymyxin B treatment)	Suzumura et al., 1998
Phosphonates	25% (^{31}P NMR)	Clark et al., 1998

[a]All values are based on surface waters (upper 100 m) unless otherwise noted.

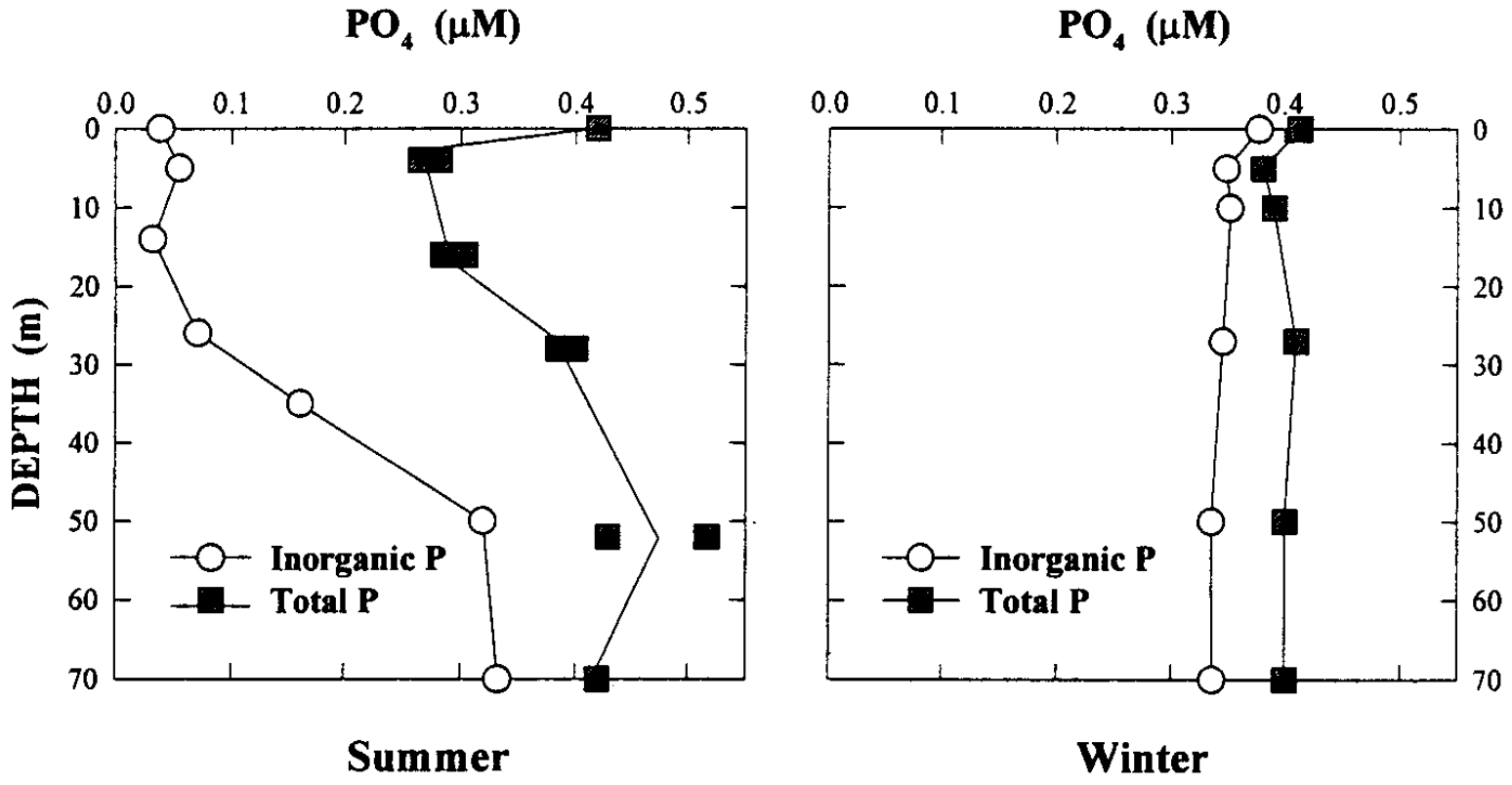

FIGURE 8.3. Typical profiles of total and inorganic phosphate in the English Channel.

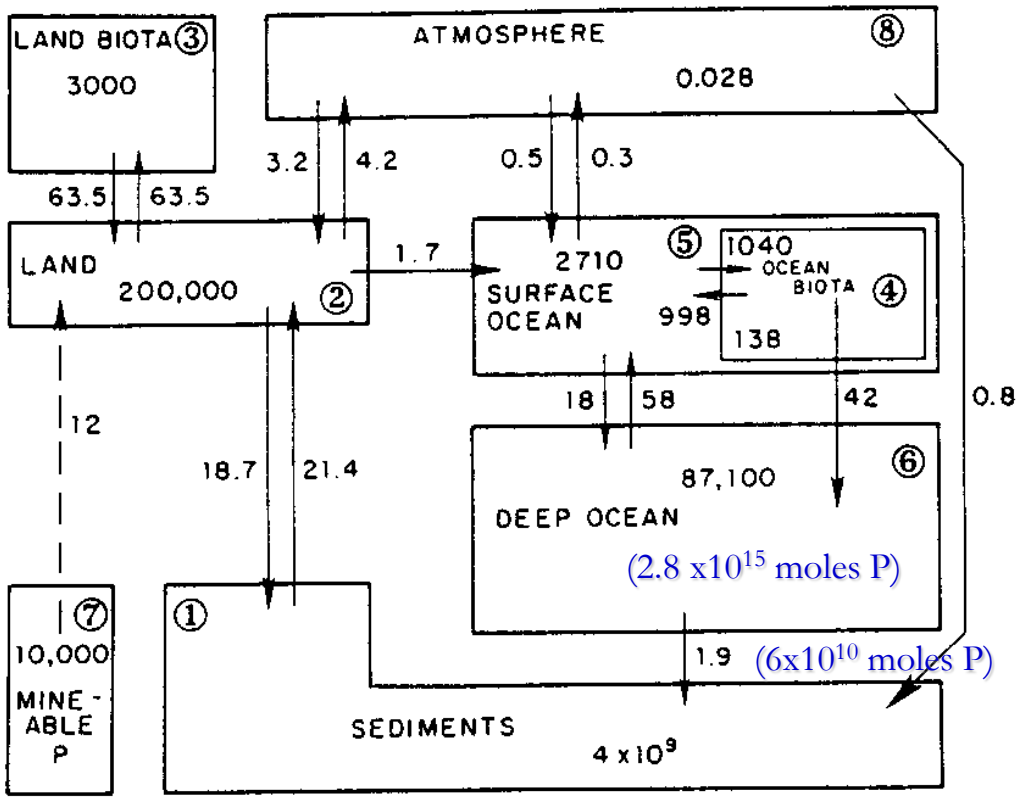

Fig. 14-7 The global phosphorus cycle. The values shown are in millions of metric tons. Reprinted from Lerman *et al.* (1975) and Graham (1977) with the permission of the Geological Society of America. See also Fig. 4-7.

Benitez-Nelson, C. R. (2000) The biogeochemical cycling of phosphorus in marine systems. *Earth-Science Reviews* 51: 109-135.

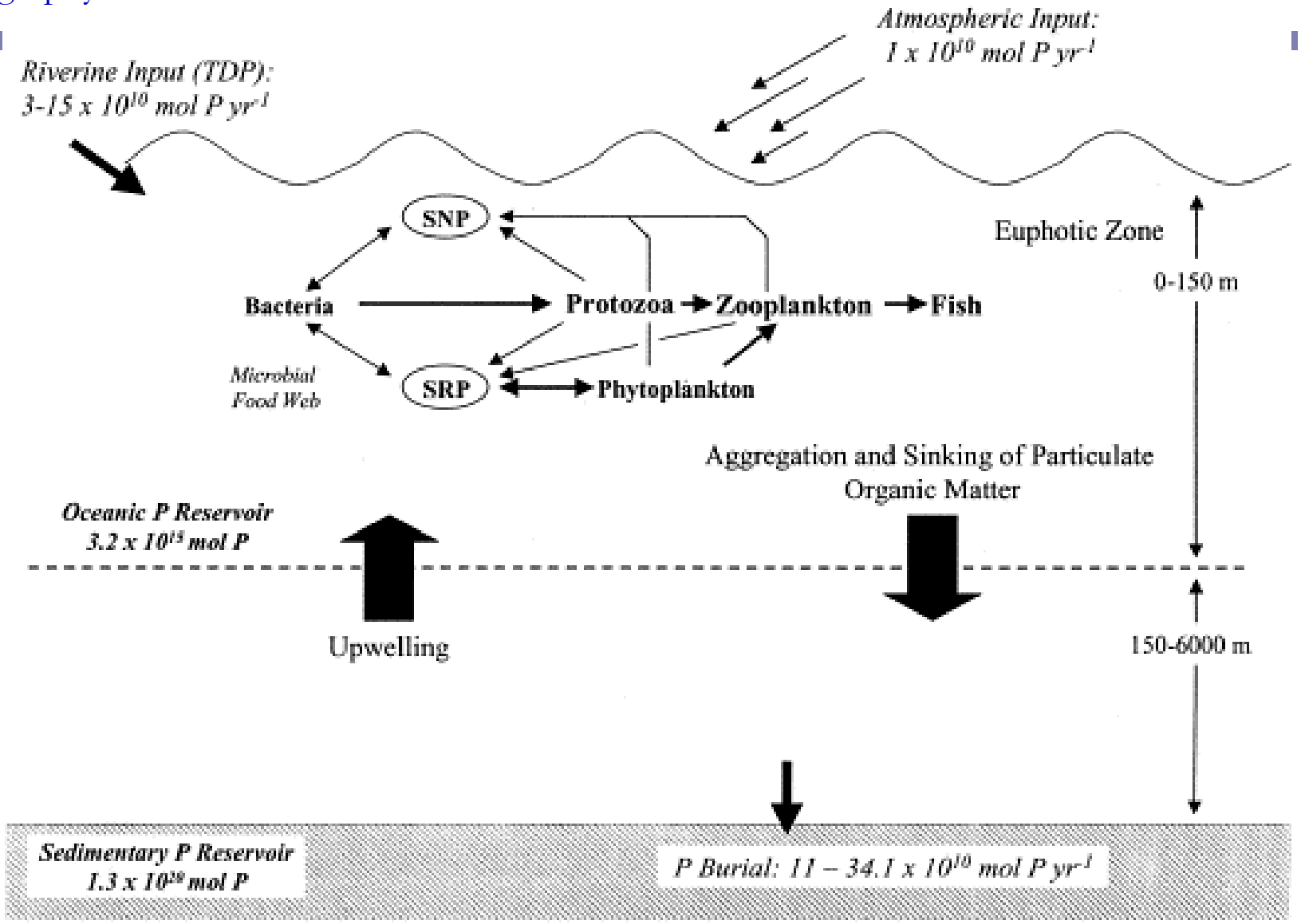

Riverine Phosphorus Flux Estimates

	Phosphorus Flux ($\times 10^{10}$ moles P/yr)	
	(a) Amazon R.	World R.
Total Dissolved P	0.3	1.6 - 3.2[1]
Releasable Solid P	0.6	3.5 - 6.0[1]
Total Reactive-P	0.9	5.1 - 9.2*

(a) after Berner and Rao., 1983.

[1]Estimate of water input to the oceans is 3.74×10^{16} liters/yr (Meybeck 1982).

*Based on pre-man global sediment transport of 7,000 to 12,000 $\times 10^{12}$ g/yr

Deep Sea vs. Continental Margin Burial Flux Estimates

Reservoir	Phosphorus Burial Flux ($\times 10^{10}$ moles P/yr)		
	[a]Deep Sea	Margin	
		max	(min)
Organic-P	1.5	4.1	(4.1)
$CaCO_3$-P	1.5	–	(–)
Iron-P	0.4	4.0	(0.4)*
Authigenic-P	0.4	9.1	(2.2)*
Loosely-sorbed-P	--	1.3	(1.3)
Total Reactive-P	3.8	18.5	(8.0)

(a) Froelich et al., 1982.
* Excludes deltaic Fe-P and background authigenic-P.

Table 1
Pre-anthropogenic marine P sources and sinks

SOURCES		
Riverine	TDP: $3–15 \times 10^{10}$ mol P yr^{-1}	Froelich et al., 1982; Howarth et al., 1995; Delaney, 1998
Atmospheric	Soluble reactive P: 1×10^{10} mol P yr^{-1}	Graham and Duce, 1979, 1981, 1982
Volcanic	Unknown, but most likely of only regional impact.	Yamagata et al., 1991; Resing, 1997
Total	$4–16 \times 10^{10}$ mol P yr^{-1}	
SINKS		
Organic matter burial	$1.1–4.1 \times 10^{10}$ mol P yr^{-1}	Froelich et al., 1982; Mach et al., 1987; Ruttenberg, 1993; Delaney, 1998
Precipitation with oxyhydroxides and clay adsorption	$1.45–5.3 \times 10^{10}$ mol P yr^{-1}	Froelich et al., 1982; Ruttenberg, 1993; Howarth et al., 1995
Phosphorite Burial	$> 8 \times 10^{10}$ mol P yr^{-1}	Ruttenberg, 1993; Filippelli and Delaney, 1996
Hydrothermal	$0.4–0.65 \times 10^{10}$ mol P yr^{-1}	Froelich et al., 1982; Wheat et al., 1996
Total	$11–34.1 \times 10^{10}$ mol P yr^{-1}	
RESIDENCE TIME	Assuming a global P inventory of 3.2×10^{15} mol P	
Maximum estimate:	20,000–80,000 years (Based on Sources)	
Minimum estimate:	9300–29,100 years (Based on Sinks)	

Ruttenberg, K. C. (1992) Development of a Sequential Extraction Method for Different Forms of Phosphorus in Marine-Sediments. *Limnology and Oceanography* 37: 1460-1482.

Ruttenberg, K. C. (1993) Reassessment of the Oceanic Residence Time of Phosphorus. *Chemical Geology* 107: 405-409.

Ruttenberg, K. C. and R. A. Berner (1993) Authigenic Apatite Formation and Burial in Sediments from Non- Upwelling, Continental-Margin Environments. *Geochimica Et Cosmochimica Acta* 57: 991-1007.

Stumm and Morgan, *Aquatic Chemistry*, 1996

Table 7.5. Equilibrium Constants Related to the Solubility of Phosphates of Fe(III), Al(III), Fe(II), and Ca^{2+}

	log K (25°C, I = 0)
$FePO_4 \cdot 2H_2O(s)$ (strengite) $= Fe^{+3} + PO_4^{-3} + 2H_2O$	−26
$AlPO_4 \cdot 2H_2O(s)$ (variscite) $= Al^{+3} + PO_4^{-3} + 2H_2O$	−21
$CaHPO_4(s) = Ca^{+2} + HPO_4^{-2}$	−6.6
$Ca_4H(PO_4)_3(s) = 4Ca^{+2} + 3PO_4^{-3} + H^+$	−46.9
$Ca_{10}(PO_4)_6(OH)_2(s) = 10Ca^{+2} + 6PO_4^{-3} + 2OH^-$	−114
$Ca_{10}(PO_4)_6(F)_2(s) = 10Ca^{+2} + 6PO_4^{-3} + 2F^-$	−118
$Ca_{10}(PO_4)_6(OH)_2(s) + 6H_2O = 4[Ca_2(HPO_4)(OH)_2] + 2Ca^{+2} + 2HPO_4^{-2}$	−17
$CaHAl(PO_4)_2(s) = Ca^{+2} + Al^{+3} + H^+ + 2HPO_4^{-3}$	−39
$CaF_2(s) = Ca^{+2} + 2F^-$	−10.4
$MgNH_4PO_4(s) = Mg^{+2} + NH_4^+ + PO_4^{-3}$	−12.6
$FeNH_4PO_4(s) = Fe^{+2} + NH_4^+ + PO_4^{-3}$	~ −13
$Fe_2(PO_4)_2(s) = 3Fe^{+2} + 2PO_4^{-3}$	~ −32

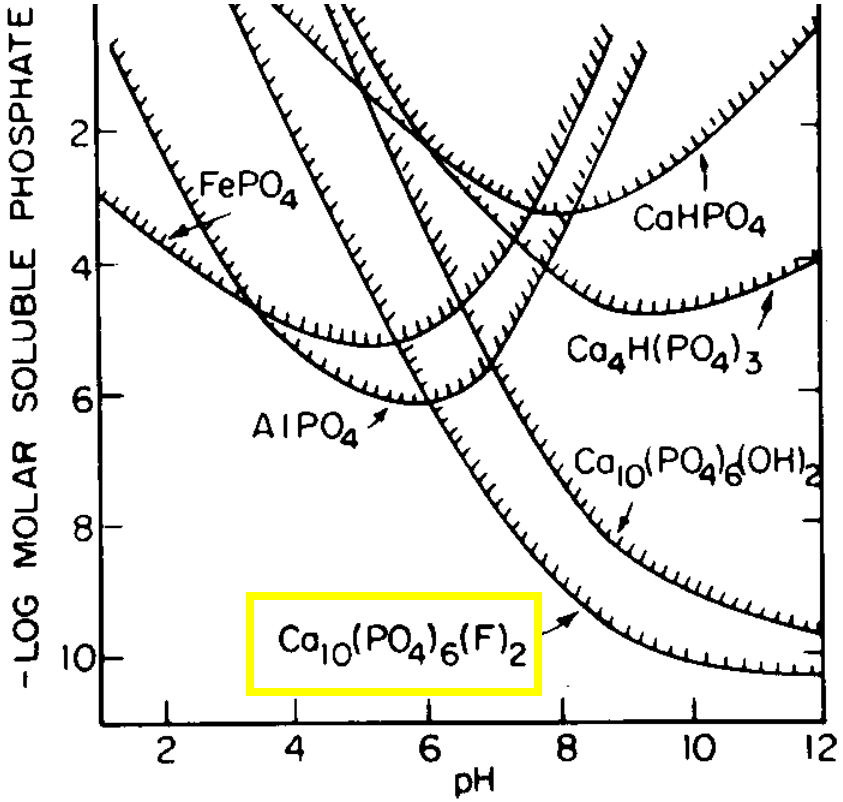

Figure 7.20. Solubility of the metal phosphates. The solubilities of $AlPO_4$ and $FePO_4$ have been calculated on the basis of the equilibria assuming that $FePO_4s(s)$ or $AlPO_4(s)$ can be converted into $Fe(OH)_3(s)$ [or α-$FeOOH(s)$ or $Al(OH)_3(s)$.] The solubility of the calcium phosphate phases has been calculated under the assumption that $[Ca^{2+}] = 10^{-3}$ M and that F^- is regulated by the solubility of $CaF_2(s)$.

Reimers, C. E., K. C. Ruttenberg, D. E. Canfield, M. B. Christiansen and J. B. Martin (1996) Porewater pH and authigenic phases formed in the uppermost sediments of the Santa Barbara Basin. *Geochimica Et Cosmochimica Acta* 60: 4037-4057.

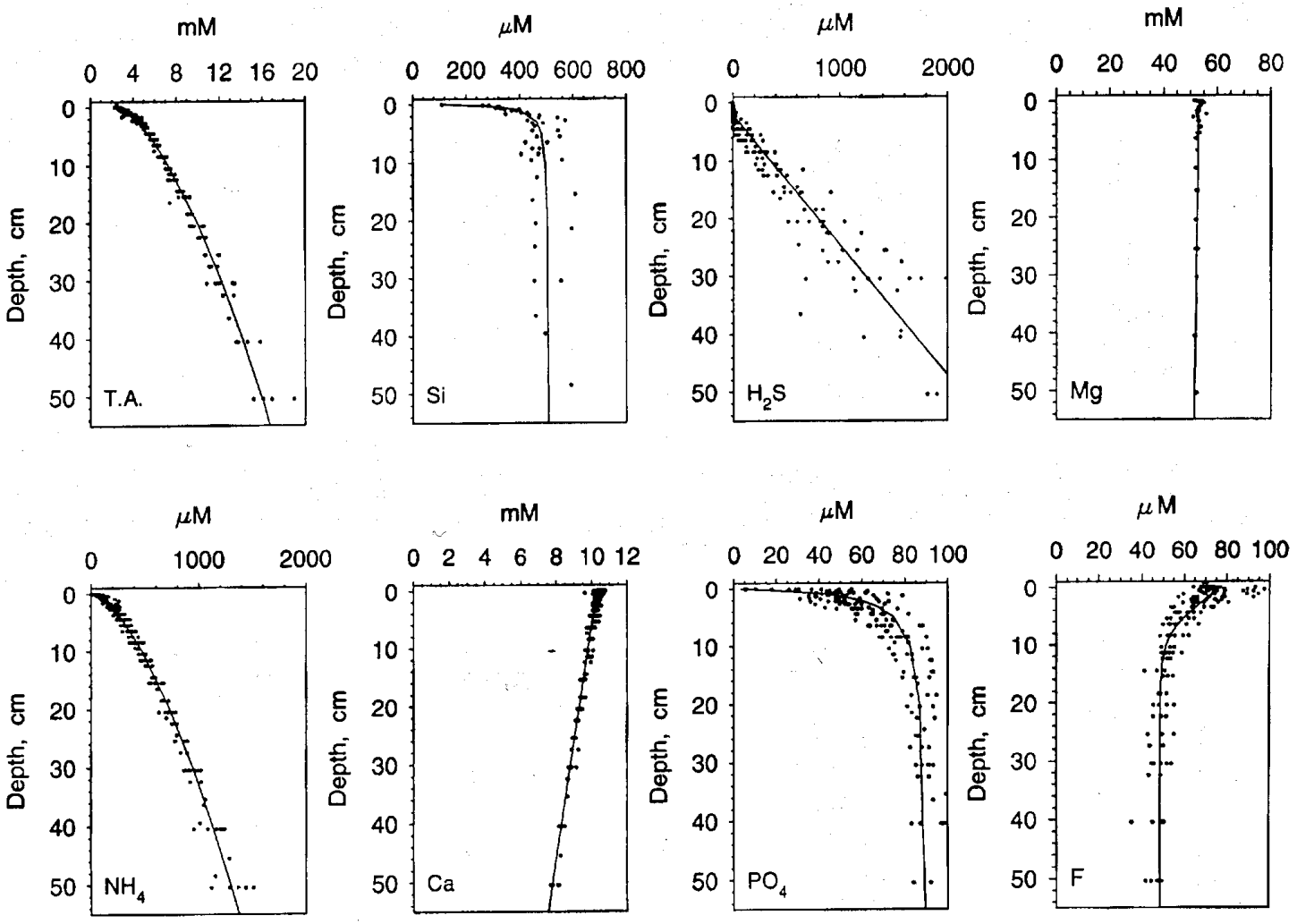

FIG. 9. Composite profiles of porewater total alkalinity, silica, hydrogen sulfide, ammonia, Ca, and phosphate taken from all the box cores analyzed. Phosphate data from BC78 and 82 are omitted. The curves through each plot represent best fits of simple functions to these data. These curves may be written as TA (mM) = $1.13x^{0.633} + 2.41$, where x = depth in centimeters; Si (μM) = $((400x)/(0.378 + x)) + 110$; H_2S (μM) = $44.2(x - 2.02)$; NH_4 (μM) = $114x^{0.622}$; Ca (mM) = $-0.0497x + 10.3$; PO_4 (μM) = $((88.0x/(1.19 + x)) + 3.70$; Mg (mM) = $-0.030x + 53.14$; and F (μM) = $37.5/(1 + e^{.355(x-2.971)}) + 48.57$.

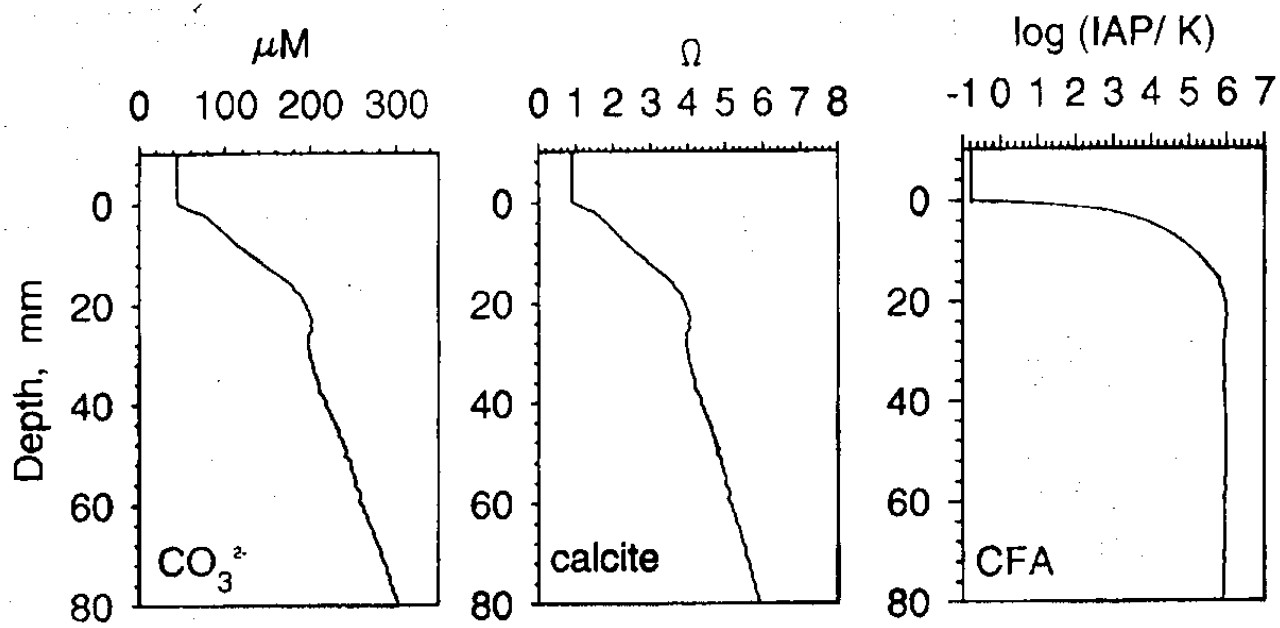

FIG. 14. Carbonate ion concentration, the degree of calcite saturation, and the ratio of the Ion Activity Product to solubility product for CFA as a function of depth in SBB sediments.

Phosphorite Deposits through Time

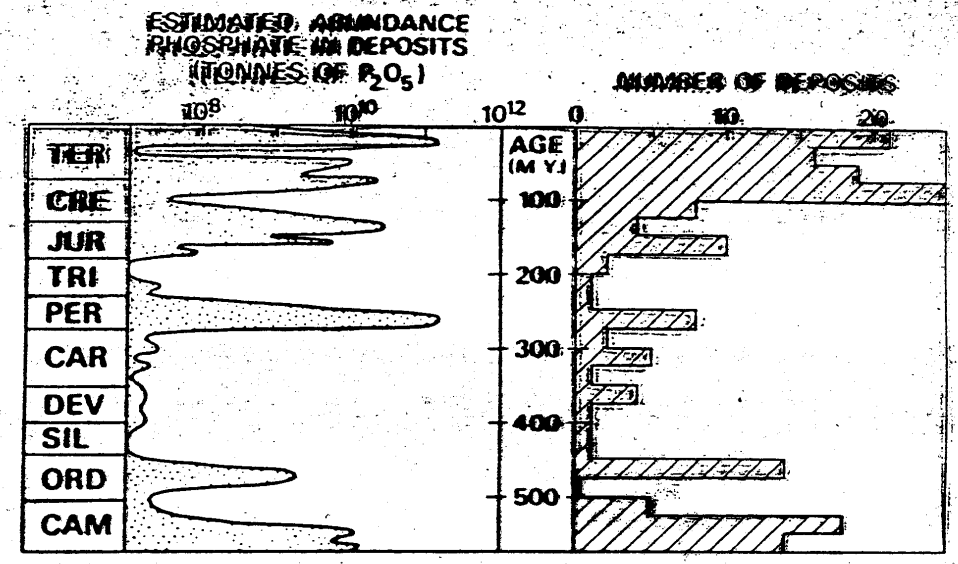

Diagnostic Indicators of CFA Formation

1. Downward decreasing pore water [F-] gradient.

2. Pore water [PO_4] decoupled from pore water [NH_4].

3. Saturation state of pore waters.

4. Identification of CFA in the solid-phase of sediments:
   - direct ID (XRD, SEM) requires >1 wt% P.
   - indirect ID via selective extraction (SEDEX) ca. 0.005 wt% P.

Krom et al. (1991)
Limnol. Oceanogr. 36,
pgs. 424-432

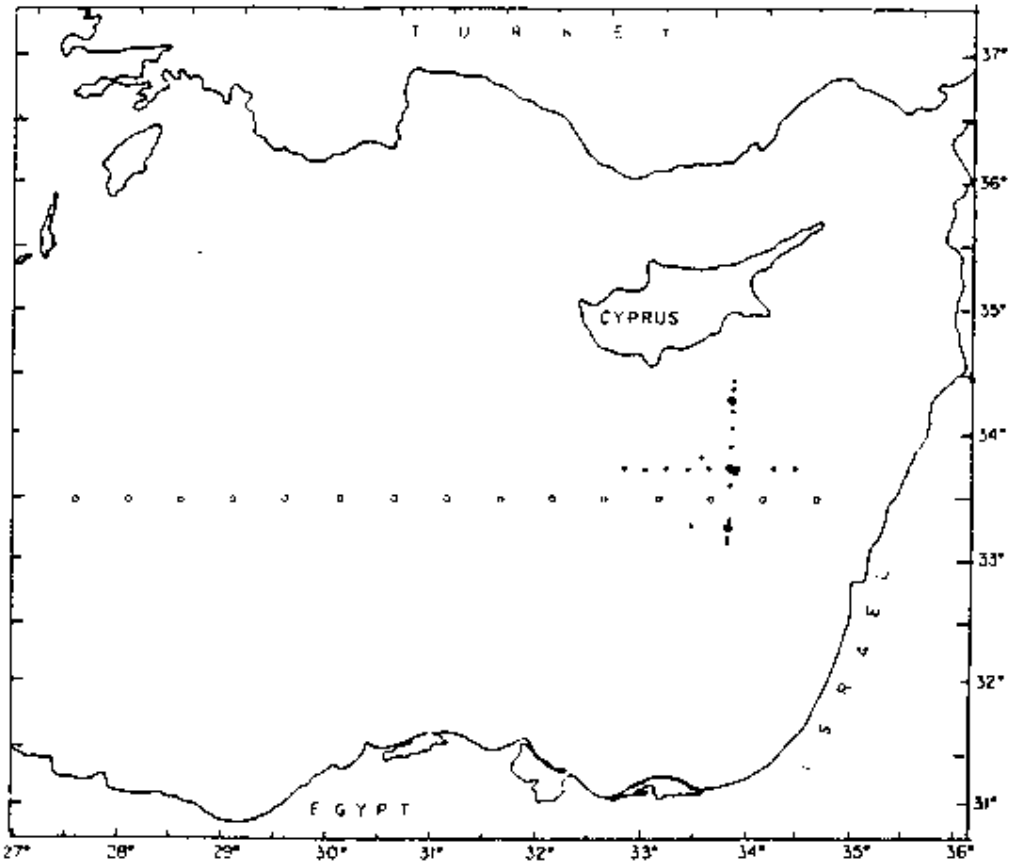

Fig. 1. Map of the southeastern Levantine basin showing the station locations used to sample the warm-core eddy in May 1989 as typical of all the eddy cruises (●) and those stations sampled across the eastern Mediterranean which have been used in this study (○).

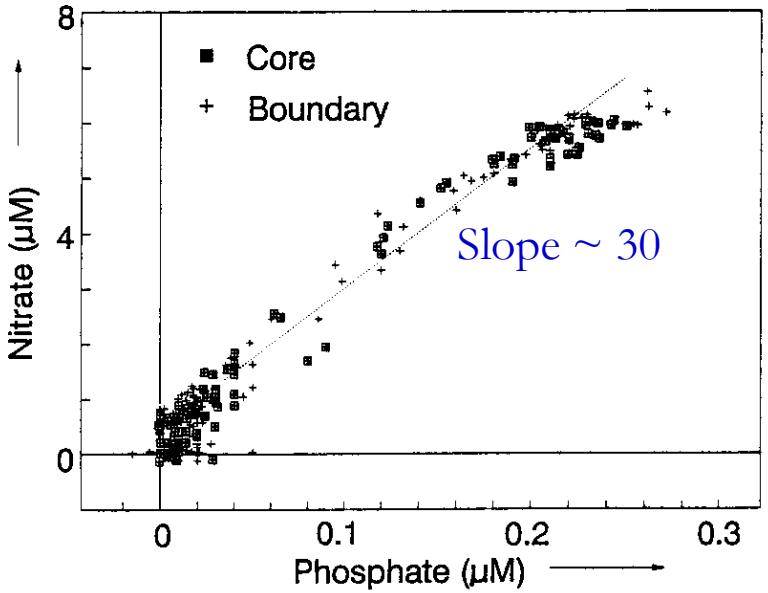

Fig. 5. NO_3^- vs. PO_4^{3-} in combined data from both the core and boundary stations of the Cyprus eddy. Data from February, May, September, and November 1989. Of the 272 data points included, 15 are from depths >1,000 m.

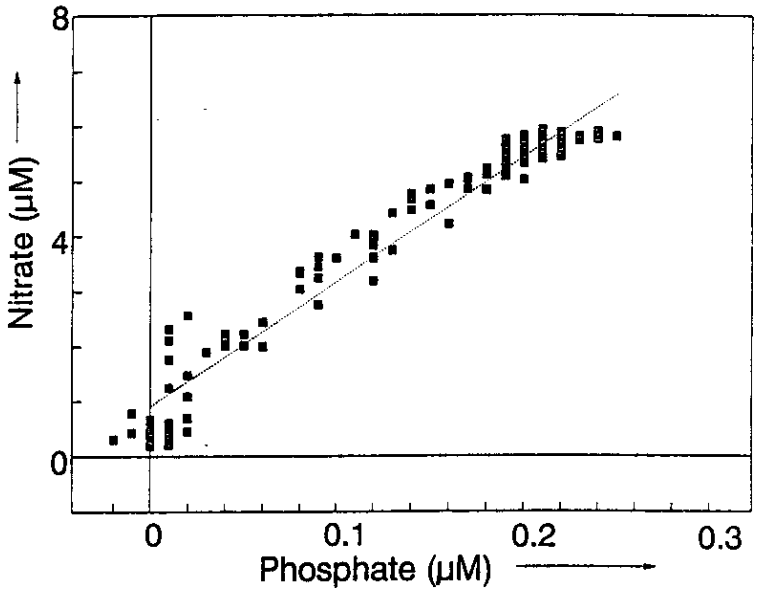

Fig. 6. NO_3^- vs. PO_4^{3-} from stations sampled across the southeastern Levantine basin at 33°30′N collected at 0.5° spacing from 34°30′E to 27°30′E. Of the 150 data points included, 10 are from depths >1,000 m.

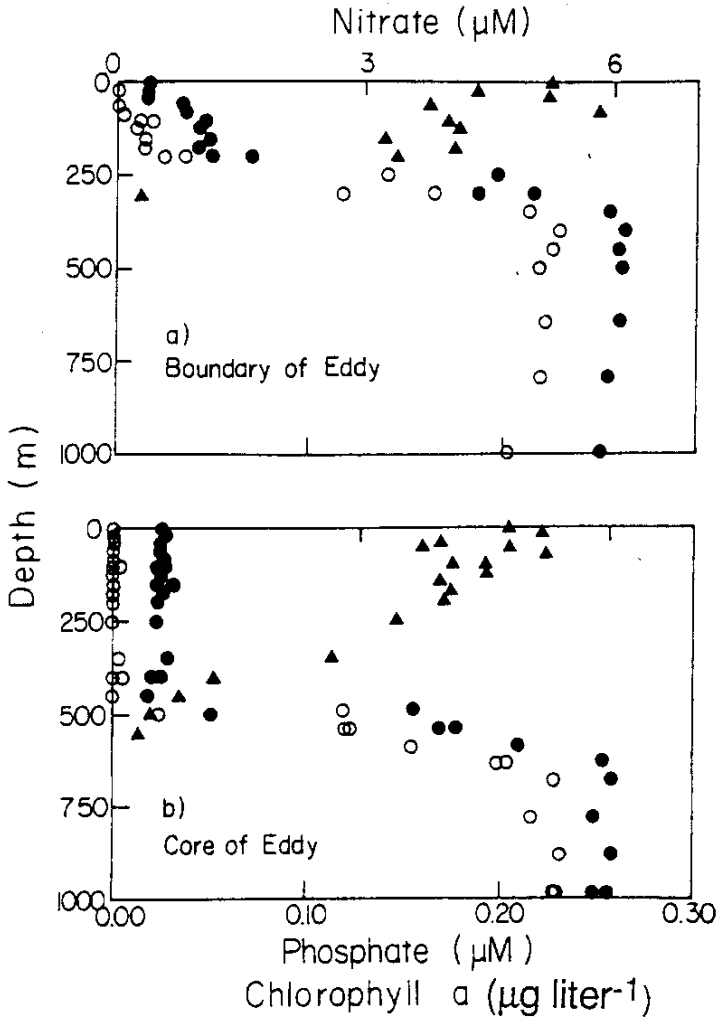

Fig. 2. NO_3^- (●), PO_4^{3-} (○), and Chl *a* (▲) vs. depth in the boundary and core stations of the Cyprus eddy sampled in February 1989.

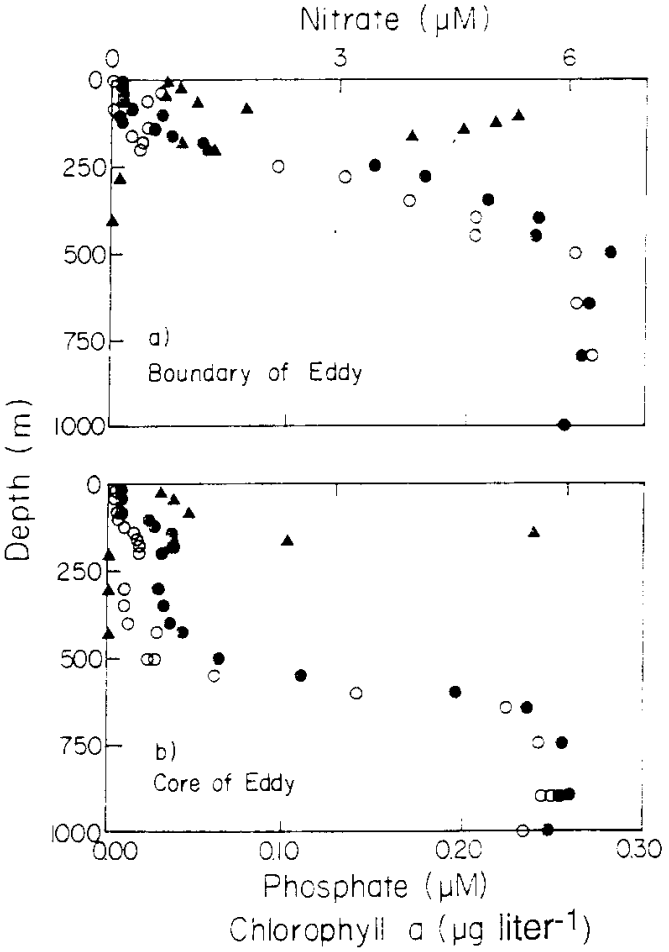

Fig. 3. As Fig. 2, but in May 1989 as typical of summer conditions.

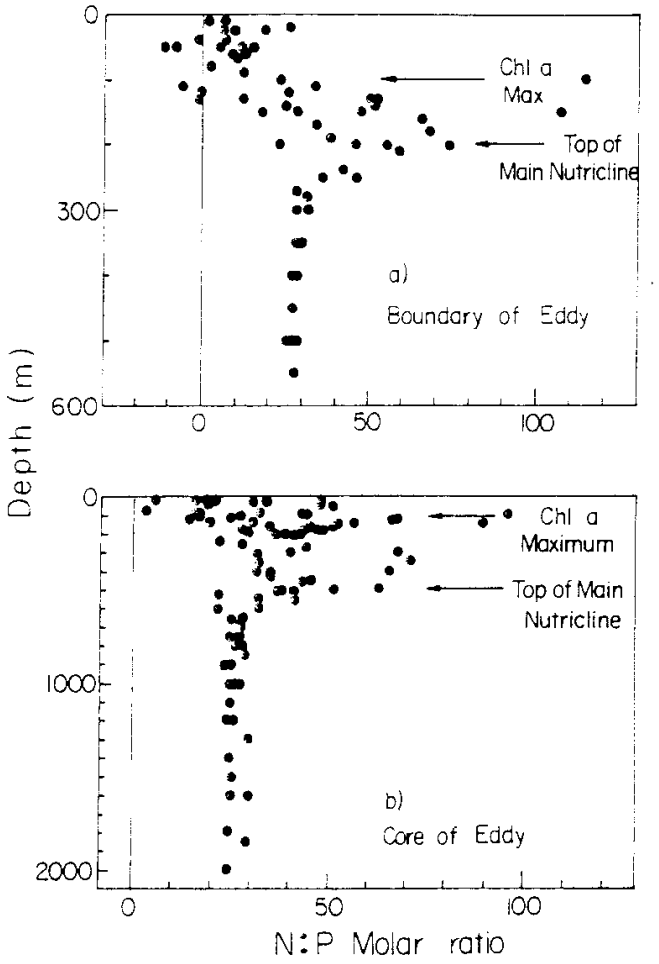

Fig. 4. N : P (NO_3^- : PO_4^{3-}) ratio vs. depth in the boundary and core stations of the Cyprus eddy. These figures combine data from May, September, and November 1989. The depth of the Chl *a* maximum and the top of the main nutricline are shown. Note the change in depth scale between panels.

800 m in the core and about constant values of 5.5 μM NO_3^- and 0.24 μM PO_4^{3-} below. In May, a surface pycnocline developed